Estonian Journal of Engineering, 2011, **17**, 3, 220–240 doi: 10.3176/eng.2011.3.04

A method for mixing molten metal and a compatible electric arc furnace

Heigo Mõlder[a], Jaan Järvik[a], Kuno Janson[a], Rauno Gordon[b] and Toomas Vaimann[a]

[a] Department of Fundamentals of Electrical Engineering and Electrical Machines, Tallinn University of Technology, Ehitajate tee 5, 19086 Tallinn, Estonia; Heigo.Molder@ttu.ee, Jaanvik@cc.ttu.ee, Kunojanson@staff.ttu.ee, Toomas.Vaimann@ttu.ee

[b] Thomas Johann Seebeck Department of Electronics, Tallinn University of Technology, Ehitajate tee 5, 19086 Tallinn, Estonia; rauno@elin.ttu.ee

Received 25 March 2011, in revised form 04 May 2011

Abstract. The objective of this paper is to study a novel method for molten metal circulation in an electric arc furnace. That involves research of operating principles, calculation methods and practical test with a pioneer prototype of the furnace. Construction of the electric arc furnace and new methods for mixing the melting metal in this furnace are described. Principles of constructing arc furnaces are specified. Calculation methods, needed for understanding the operation of the furnace are presented. Emphasis is put on the magnetic field and circulation force density calculation. Modelling of the arc furnace and of the involved processes is carried out. Testing of the pioneer prototype is described and the test results are presented. Evaluation of theoretical calculation methods is done by comparing the results with the practical data.

Key words: electric arc furnace, molten metal circulation, metal mixing, magnetic field, electric field, force, simulation.

1. INTRODUCTION

Electric arc furnaces are widely used in steel making and in smelting of non-ferrous metals. The electric arc furnace is the central part of the so-called mini-mills, which produce steel mainly from scrap. Typical electric arc furnaces operate at power levels from 10 to 100 MW [1].

Technical literature and patent research reveal that DC furnaces have a number of advantages when compared to AC furnaces. These advantages include power quality, stability of the melting process and smaller wearing of electrodes per a ton of melted metal [2]. Main disadvantage of DC furnaces is that the quick and effective mixing of the molten metal is hard to achieve.

In case of AC furnaces, currents induced from line voltages close in the molten metal and create a 50 Hz magnetic field that changes in time. This magnetic field induces electromotive force in the metal which in turn induces eddy currents. Secondary magnetic field of eddy currents joins with the primary magnetic field of line currents and creates a force that facilitates the mixing of liquid metal.

In case of AC furnaces, the mixing process cannot be controlled and the forces that are created by joining the eddy current magnetic fields, 50 Hz time varying magnetic field and induced electromotive forces, are not in accordance with the weight of the molten metal that has to be mixed. Due to this the mixing efficiency is not sufficient.

To make the mixing process in the DC furnace possible, we add AC component to the DC component (Fig. 1) and investigate the emerging mixing forces on particular frequencies. To simplify the picture of primary electro-magnetic fields and to change it to be more oriented to a specific direction, research is carried out for the solution where electrodes of the furnace are being supplied by three independent sources, so that the currents that are passing the molten metal would evolve straight from the lower electrodes to the upper ones. This solution is needed to make the mixing process in the furnace controllable.

Supply voltages can be calculated using the following formulas:

$$e_A = E_a + E_m \sin \omega t, \tag{1}$$

$$e_B = E_a + E_m \sin(\omega t + 120°), \tag{2}$$

$$e_C = E_a + E_m \sin(\omega t + 240°), \tag{3}$$

where E_a is the DC component of the supply voltage, E_m is the AC component of supply voltage and ω is the angular frequency, calculated as $\omega = 2\pi f$, where f is frequency, and t is time.

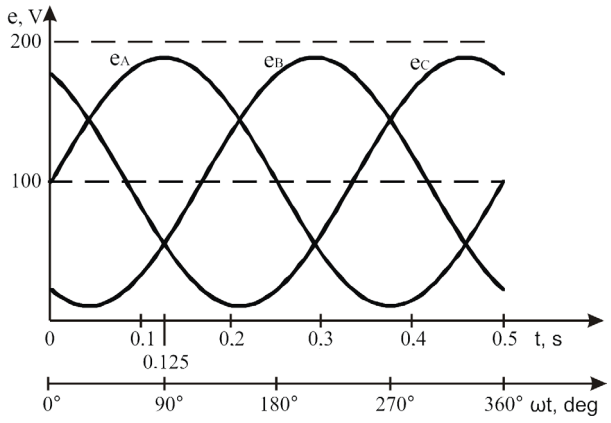

Fig. 1. Change of the source electromotive forces on supply frequency 2 Hz.

1.1. Physical model of the arc furnace

Figure 2 shows the scheme of the electric arc furnace. In this particular model, there are three electrodes that are moved vertically up and down with hydraulic actuators. In the beginning of the melting process, when the metal is still in solid state, only DC voltage is used. When the metal has melted and is already in the liquid state, AC component is added to supply voltage [3].

The arc furnace for mixing the molten metal (Fig. 2) consists of a bath 1, in which the molten metal 2 is kept. Above the furnace bath are the upper electrodes 3.1, 3.2 and 3.3 that are shifted in space for an angle 120° between each other, and under the bottom of the furnace are the lower electrodes 4.1, 4.2 and 4.3. Electrodes are supplied from the supply grid through electrode sources 5.1, 5.2 and 5.3. Electrode sources get their supply from the grid 6. Control system 7 is used to control the arc furnace and it consists of three source control devices 8.1, 8.2 and 8.3, power regulator of the arc furnace 9 and the control device for the mixing process of molten metal 10. The latter includes a device 11 for forming the mixing signals, mixing frequency generator 12, a device for forming the mixing current amplitude signal 13 and a device for forming the signal of phase sequence 14.

1.2. Parameters of geometrical dimensions and materials

An arc furnace with electrode diameter of 0.27 m and upper electrode length of 0.5 m has been constructed as a starting model for modelling calculations. The upper electrodes are made short intentionally to reduce the amount of numerical field calculations. Length of the lower electrodes is 0.3 m and the total weight of the molten metal in the furnace is about 50 t. Geometrical dimensions of the arc furnace are shown in Table 1 and the parameters of chosen materials in Table 2.

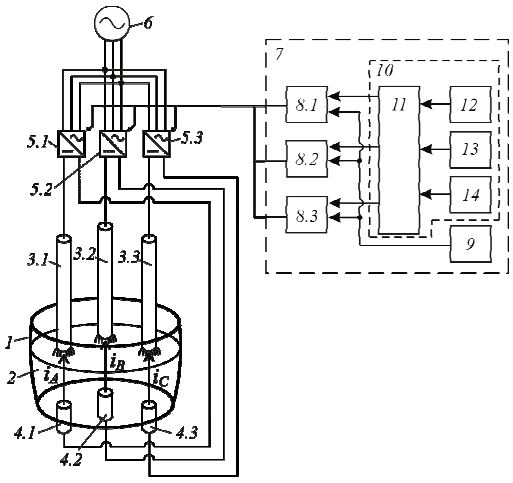

Fig. 2. Scheme of the arc furnace.

Table 1. Geometrical dimensions of the arc furnace

Name of geometric dimension	Numerical value
d_E – electrode diameter	0.27 m
S_E – area of cross section of the electrode	0.058 m^2
l_E – electrode length	0.5 and 0.3 m
d_{m1} – upper diameter of the molten metal in the furnace	3.4 m
d_{m2} – lower diameter of the molten metal in the furnace	2.4 m
l_m – height of the molten metal	0.9 m
Total weight of the molten metal	50 t

Table 2. Parameters of chosen materials

Molten metal parameters	Numerical value
ρ – density of the molten steel	7850 kg/m^3
T – temperature of the molten steel	1873 K
v – kinematic viscosity of the molten steel	1 m^2/s
σ_1 – conductivity of the molten steel in the ladle	1.04×10^6 S/m
Graphite electrode parameters	**Numerical value**
ρ – density of the graphite electrode	1950 kg/m^3
σ_2 – conductivity of the graphite electrode	3×10^3 S/m

During the assembly of the model, the slag layer that forms on the surface of the molten metal is discarded to simplify the modelling calculations, because its diameter and resistance vary depending on the alloying components that are added and on the time of the melting process. Also the resistance of the arc between electrodes and molten metal is discarded, as this value too varies in great limits. For checking the reliability of the furnace, those two components are not important at the moment.

1.3. Solving the electrical circuit of the electric arc furnace

To solve any electrical model, assumptions are made to facilitate the derivation. Similarly, the electric arc furnace electrical circuit requires several assumptions before reaching the final equations. The first step in the analysis of the electrical circuit is to use the Kirchhoff current law (KCL) to equate currents and voltages.

Figure 3 shows that every electrode pair has its own independent supply source. It means that the current trajectory in the molten metal can close only in the limitations of one source, so the currents flow from lower electrodes to opposite upper electrodes.

To calculate the currents that are flowing through the molten metal, conductivity of the molten metal has to be taken into account (Table 2).

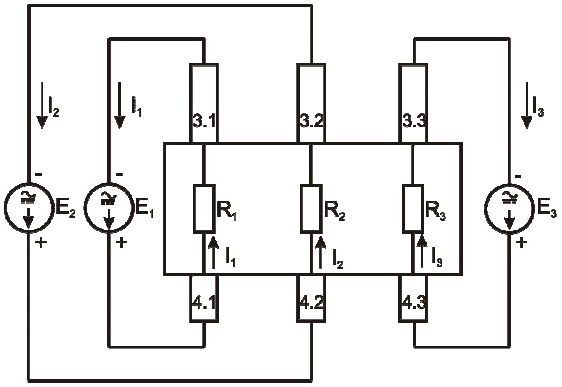

Fig. 3. Principle scheme of the arc furnace.

To simplify the modelling of the arc furnace and check its reliability, the parameters of the slag and arc are discarded.

Firstly, resistances of the electrode and molten metal are calculated using the following formula:

$$R = \frac{\rho l}{S}, \tag{4}$$

where R is the resistance of the electrode or molten metal (Ω), ρ is the resistivity of the electrode or molten metal (Ωm) and S is the area of the cross-section of the electrode or molten metal (m^2).

Calculations show that the resistance of the molten metal in the bath is $R_m = 1.22 \times 10^{-7}\ \Omega$ and the resistance of the electrode is $R_E = 4.59 \times 10^{-3}\ \Omega$. When resistances of the electrodes and molten metal are known, the next step will be to calculate the currents of the arc furnace. Currents depend from the supply voltage. In the beginning of the melting process, the supply is switched only to DC voltage U_a and when the metal is already melted, AC component U_m is added to the DC component. Dimension and frequency of the AC component has to be selected so that the mixing efficiency would reach its maximum value. These parameters depend on the parameters of the metal to be melted and the construction of the arc furnace. Chosen values of supply voltages are shown in Table 3.

Table 3. Chosen values of supply voltages

Variables	Acceptable range	Chosen value
U_a – DC component of the supply voltage	100–1000 V	100 V
U_m – AC component of the supply voltage	$0 \le U_m \ge U_a$	85 V
f – supply frequency	0–50 Hz	2 Hz
Shift between three phases	120°	120°

After completing the resistance calculation it is possible to calculate the instantaneous values of arc furnace currents using the following formulas:

$$i_1 = \frac{U_a + U_m \sin(\omega t + 0°)}{R_m + R_E}, \tag{5}$$

$$i_2 = \frac{U_a + U_m \sin(\omega t + 120°)}{R_m + R_E}, \tag{6}$$

$$i_3 = \frac{U_a + U_m \sin(\omega t + 240°)}{R_m + R_E}. \tag{7}$$

Observing at $t = 0.125$ s at 90° with supply frequency of 2 Hz, the instantaneous values of the current will be $i_1 \cong 40$, $i_2 \cong 12.5$ and $i_3 \cong 12.5$ kA. In fact, currents depend very much on the depth of the electrode in the slag layer. Length of the arc and the resistance of the slag depend on this as well. In the given case the electrodes are in connection with the molten metal and in that case the currents have the values shown above. Relying on currents and voltages gives the opportunity to calculate the whole power of the arc furnace, which is 8.9 MW. If the power is kept constant and the slag as well as arc resistances are taken into account, evidently the supply voltage has to be risen.

1.4. Governing equation for calculating electromagnetic forces

Maxwell's I law describes the dependence of magnetic field intensity vector $\vec{B}$ on the current density $\vec{J}$

$$\Delta \times \vec{H} = \vec{J}. \tag{8}$$

According to Maxwell's II law, vector of the electrical field strength $\vec{E}$ (V/m) depends on the changing speed of the magnetic flux density $\vec{B}$

$$\Delta \times \vec{E} = -\frac{\partial \vec{B}}{dt}. \tag{9}$$

Field dimensions can be linked with each other using the equations

$$\vec{B} = \mu \vec{H}, \tag{10}$$

$$\vec{J} = \sigma(\vec{E} + (\vec{U} \times \vec{B})), \tag{11}$$

where μ is magnetic permeability (H/m) and $\vec{H}$ is magnetic field density (A/m), σ is electrical conductivity (S/m) and $\vec{U}$ is velocity of the conductor in the magnetic field. The Lorentz force $\vec{F}$, due to interaction of the electro-magnetic fields, is given by

$$\vec{F} = \vec{J} \times \vec{B}. \tag{12}$$

To determine the electromagnetic force, it must first be decided whether to solve $\vec{J}$ or $\vec{B}$ in the conducting domain, because $\vec{J}$ and $\vec{B}$ are linked to each other by Eqs. (8) and (11).

From the above equations we can derive a differential equation for $\vec{B}$

$$\frac{\partial \vec{B}}{\partial t} = \frac{1}{\sigma\mu}\nabla^2 \vec{B} + \nabla \times \vec{U} \times \vec{B}. \tag{13}$$

Since the magnetic Reynolds number is low in this metallurgical process, the second term on the right side of Eq. (13) can be neglected [4]. Thus Eq. (13) reduces to

$$\frac{\partial \vec{B}}{\partial t} = \frac{1}{\sigma\mu}\nabla^2 \vec{B}. \tag{14}$$

This is a magnetic diffusion equation. In steady state the equation reduces to an elliptic partial differential equation. The above magnetic diffusion equation is now solved with the appropriate boundary conditions to obtain the values of $\vec{B}_x$, $\vec{B}_y$, and $\vec{B}_z$. With the help of the magnetic fields, the induced current density can be calculated by Eq. (8) [5].

Since the electromagnetic field is varying sinusoidally with time, it is necessary to represent the Lorentz force in Eq. (12) in the time-averaged form. The components of the Lorentz forces in x, y and z directions are given as

$$\vec{F}_x = \vec{J}_y \vec{B}_z - \vec{J}_z \vec{B}_y, \tag{15}$$

$$\vec{F}_y = \vec{J}_z \vec{B}_x - \vec{J}_x \vec{B}_z, \tag{16}$$

$$\vec{F}_z = \vec{J}_x \vec{B}_y - \vec{J}_y \vec{B}_x. \tag{17}$$

In order to compute the velocity profile in the liquid metal bath, the Lorentz forces calculated above are used as the source term to solve the incompressible Navier–Stokes equation [5].

2. MESH SETTING FOR THE THREE-DIMENSIONAL MODEL

For applying the FEM method, the investigated object is divided into finite sub-objects (Fig. 4). The FEM model is made using 8833 elements and 18 715 degrees of freedom. In electrode contact areas, where the current density is higher, also the mesh density is raised. As FEM is calculated by computer software, the main task is to specify the elements of the magnetic circuit and the parameters of magnetic fields as accurately as possible. Also the dimensions of sub-objects must be specified. The more sub-objects there are, the more accurate calculation results can be obtained, but more objects means also more needed computing power and time to complete the calculation process.

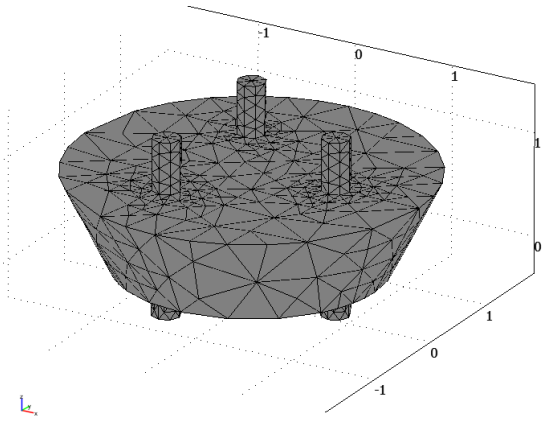

Fig. 4. Mesh for FEM calculations.

To investigate the three-dimensional fields of the arc furnace, the first step must be the drawing of the arc furnace elements in a three-dimensional way. For simplification of the calculation process, the smallest number of elements must be specified, at which the values of electrical fields, magnetic fields and forces are sufficiently accurate.

All FEM models, meshes and calculations were performed with the Comsol Multiphysics 3.5 software AC/DC Electric and Induction Current model.

2.1. Three-dimensional current density calculation

At first, current density in electrodes at $t = 0.125$ s is observed. At that moment one electrode has maximum voltage value and two other electrodes have a lower, but equal supply voltage. Figure 5 shows that current contours are closing

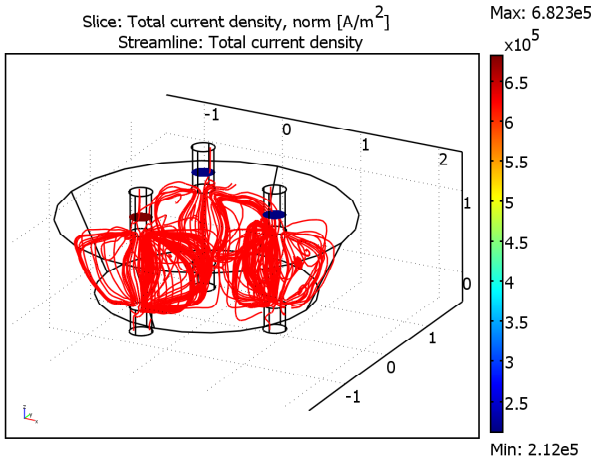

Fig. 5. Distribution of the current density in electrodes and current contours through the molten metal.

straight from lower electrodes to the upper ones. If current density $J_1 = 6.82 \times 10^5$ A/m^2 is multiplied by the area of the electrode $S_E = 0.058$ m^2, current is calculated, which correlates with the calculations using Eqs. (5), (6) and (7).

From Fig. 6 it can be observed that most of the current flows straight from lower electrodes to upper electrodes reaching the highest density just under the electrode. When the area in the middle of the molten metal is calculated, also the currents can be calculated and they correlate with the calculations mentioned before.

It can be seen from Fig. 6 that density of the primary current $J_1 = 5.79 \times 10^4$ A/m^2, with frequency of 2 Hz at the time moment $t = 0.125$ s induces secondary current density $J_2 = 461.579$ A/m^2 in the molten metal, which is shown in Fig. 7.

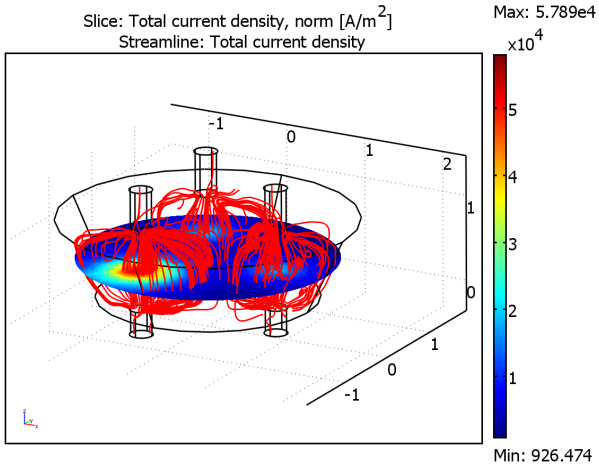

Fig. 6. Distribution of the current density and current contours through the molten metal.

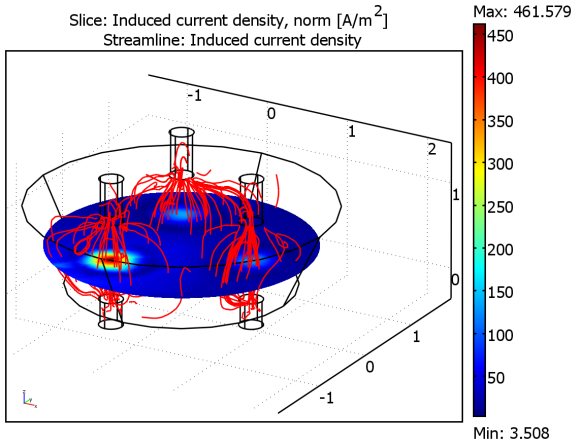

Fig. 7. Induced current densities.

2.2. Distribution of the electric field

Figure 8 shows the electric fields in the molten metal at given currents. Vectors of the electric fields have same directions as the vectors of the current density. In the first solution (Fig. 3) an assumption was made that current in the molten metal flows in the direction from below upwards. Figure 6 gave a more realistic view that is similar to the distribution of the electric field in Fig. 8. To make the figure easier to read, electric fields, emerging on the surface of the electrodes, are discarded, so that the field lines of the electric fields within the molten metal can be shown in a clearer way. Another thing to keep in mind is that electric fields shown in the figure are the summary electric fields. This means that the secondary counter electric field is separated from the primary electric fields (electric fields created by the electrodes).

2.3. Distribution of the magnetic field in case of two-dimensional calculation

First, the distribution of the magnetic field density in top view at the time moment $t = 0.125$ s at 2 Hz frequency is observed. To investigate the distribution of the magnetic field density B in the whole cross-section of the molten metal, three lines must be drawn over the cross-section, on which the magnetic field density can be observed.

In case of the magnetic field density calculations in Fig. 9 it has to be noted that it is a very simplified model, which means that the currents flow in a straight line in direction from below upwards and the field lines of the current density do not bloat. In other words, magnetic field density near the electrode is a few times higher then in case of three-dimensional calculations. However, the two-dimensional magnetic field density calculation gives a simplified image of the

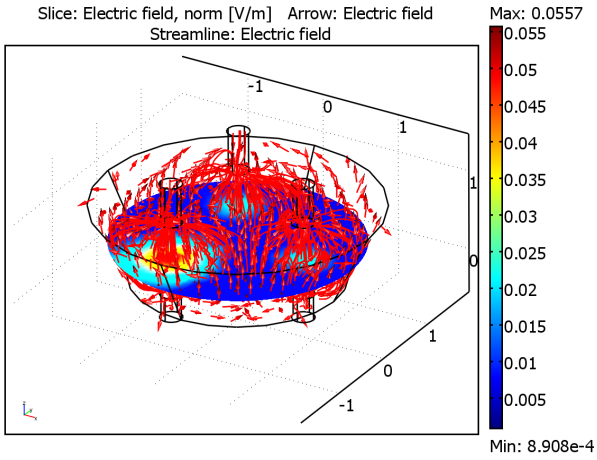

Fig. 8. Distribution of the electric field in the molten metal.

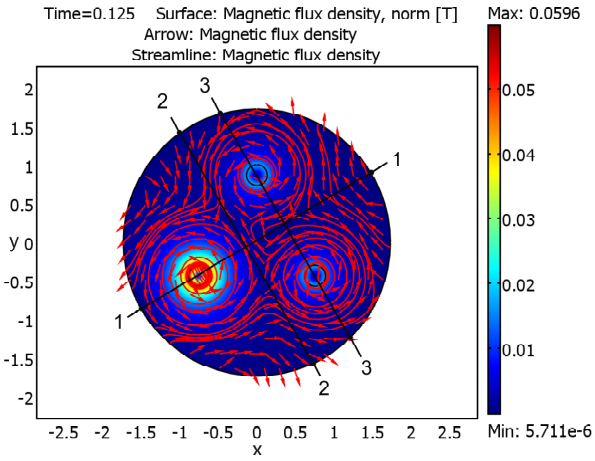

Fig. 9. Distribution of magnetic field density *B* in case of two-dimensional calculation.

distribution of the magnetic field density and the calculation process requires less computing power.

Next, the distribution of the magnetic field density B is observed on lines 1, 2, and 3. As shown in Figs. 10, 11, and 12, the magnetic field density B descends practically to 0. This is because of the skin effect, which depends on the frequency of the supply voltage [6]. Depth of the skin effect δ can be calculated as

$$\delta = \frac{1}{\sqrt{\pi\mu\sigma f}}, \tag{18}$$

where μ is the permeability of the vacuum ($4\pi\times10^{-7}$ H/m), σ is the electrical conductivity (S/m) and f is the frequency (Hz) [7].

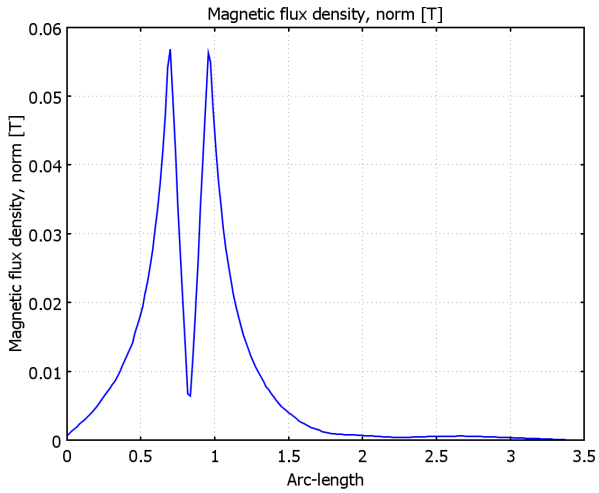

Fig. 10. Distribution of the magnetic field density *B* on line 1 (Fig. 9).

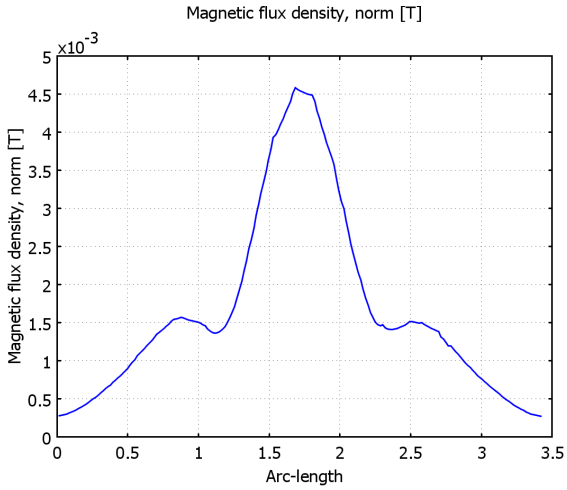

Fig. 11. Distribution of the magnetic field density *B* on line 2 (Fig. 9).

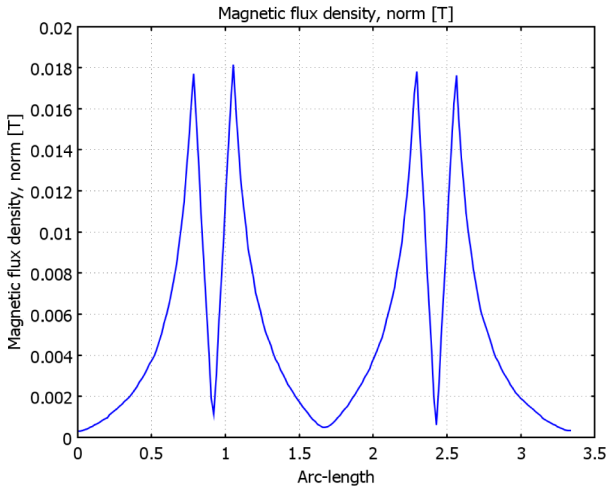

Fig. 12. Distribution of the magnetic field density *B* on line 3 (Fig. 9).

Change of the magnetic field density, integrated over time $t = 0–0.5$ s is shown in Fig. 13.

2.4. Distribution of the magnetic field in case of three-dimensional calculations

After two-dimensional magnetic field calculations we must look at the three-dimensional magnetic field calculations (Figs. 14–16). First we look at the norm of the magnetic field density B on line 1 as shown in Fig. 9.

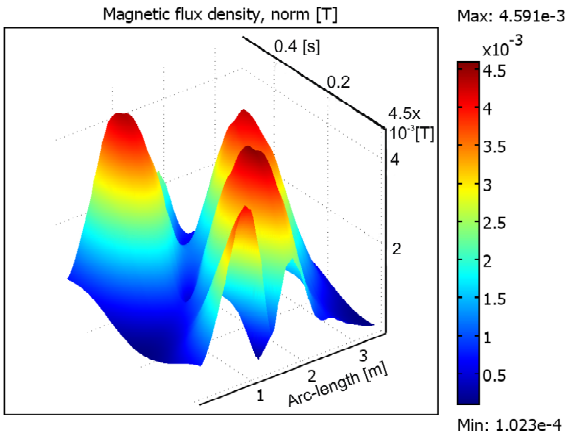

Fig. 13. Change of the magnetic field density, integrated over time t = 0–0.5 s as shown in Fig. 9.

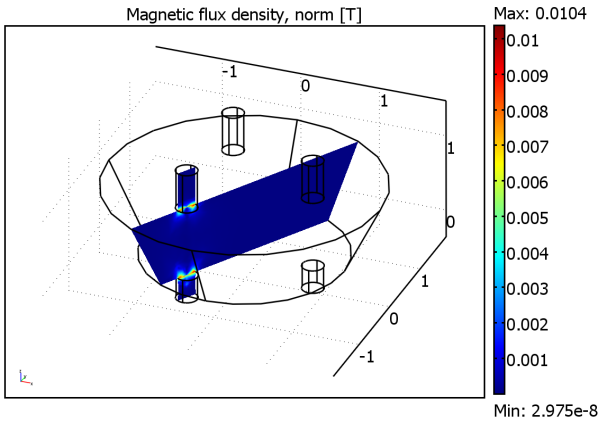

Fig. 14. Norm of the magnetic field density on line 1 (Fig. 9) at time moment t = 0.125 s.

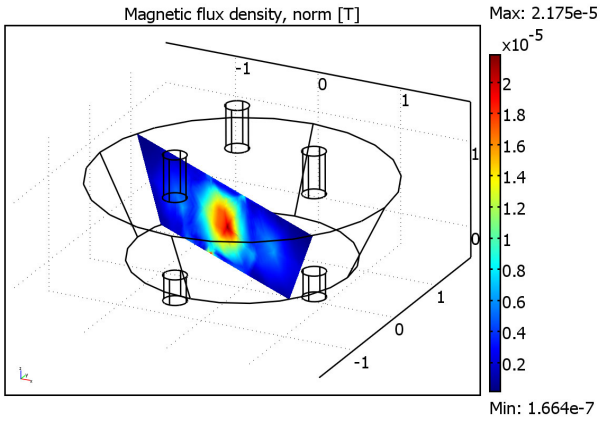

Fig. 15. Norm of the magnetic field density on line 2 (Fig. 9) at the time moment t = 0.125 s.

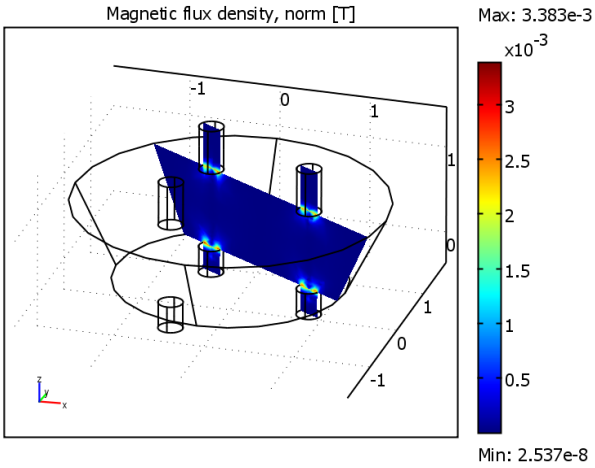

Fig. 16. Norm of the magnetic field density on line 3 (Fig. 9) at the time moment $t = 0.125$ s.

In case of three-dimensional magnetic field density calculations it can be seen that the magnetic field density is significantly smaller than in case of two-dimensional calculations. It can be explained by the fact that in case of three-dimensional calculations some part of the magnetic field emerges in the Z plane, and secondly, currents do not flow in the direction upwards as in case of two-dimensional calculations. Currents are distributed in the whole volume of the molten metal as shown in Fig. 6. Maximum normal component of the magnetic field density $B = 0.01$ T arises at the edges of the electrodes, because the edges have a maximum current density due to the skin effect.

2.5. Three-dimensional calculations of the Lorentz force

Using Eqs. (15), (16) and (17), the Comsol Multiphysics 3.5 AC/DC module – Electric and Induction Current (emqav) software has the ability to calculate force density vectors using FEM. These formulas give good results if magnetic field density B and current density J at a certain point in space have been calculated in advance. Current densities at the time moment $t = 0.125$ s and frequency 2 Hz have been calculated (Figs. 17–19).

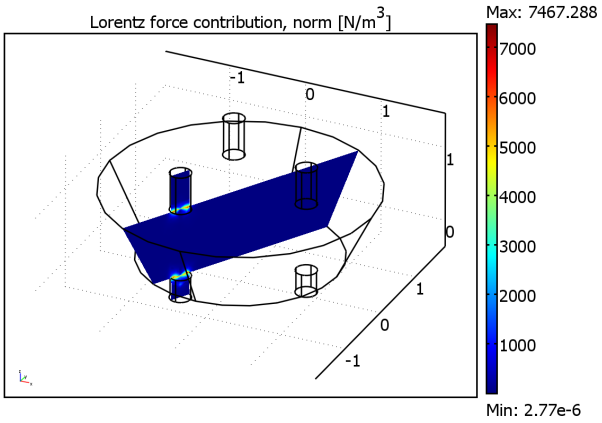

Fig. 17. Norm of the force density distribution on line 1 (Fig. 9).

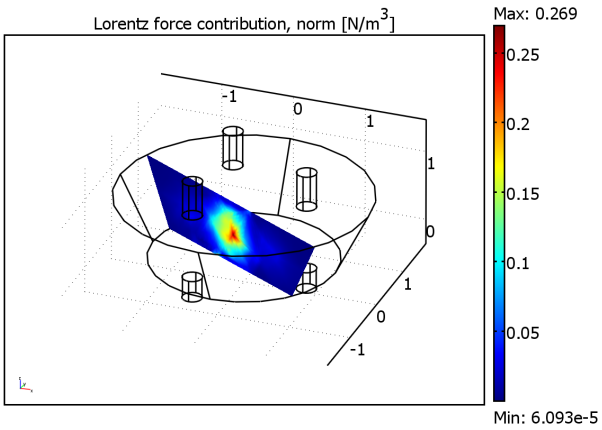

Fig. 18. Norm of the force density distribution on line 2 (Fig. 9).

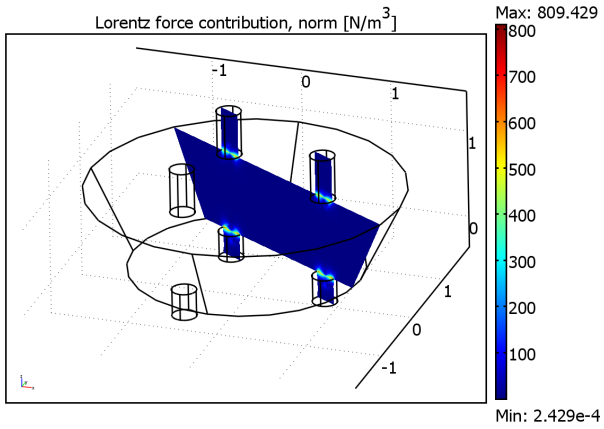

Fig. 19. Norm of the force density distribution on line 3 (Fig. 9).

3. FIRST TESTS OF THE PIONEER EXPERIMENTAL SET-UP

First experimental set-up (Figs. 20, 21) was constructed in a simplified form at the scientific laboratory of Tallinn University of Technology, Department of Fundamentals of Electrical Engineering and Electric Machines. Main parameters of the arc furnace were chosen according to existing equipment. Maximum power of the arc furnace, according to the used frequency converter, was chosen equal to 3.1 kW with nominal frequency in the range of 0–50 Hz. Lower diameter of the furnace was 120 mm, upper diameter 150 mm, and height 130 mm. Distance of the electrodes from the furnace centre was chosen equal to 50 mm. Diameters of the mentioned electrodes were 10 mm. Schematic of the experimental set-up is shown in Fig. 20. A number of simplifications were made:

1) it was impossible to use higher currents;
2) transformer was used as independent supply source, thus the tests were carried out at the frequency of 50 Hz;
3) tests were carried out using AC voltage;
4) salt solution with resistivity of 0.84 Ωm was used instead of the molten metal.

First test was made using 50 Hz supply voltage with total current of 3.5 A. Fan, attached to a string, was lowered into the salt solution as shown in Fig. 22 and turning velocity of the fan in the salt solution was measured at different heights. Velocity of the fan at such current and frequency was about 1.6 rpm.

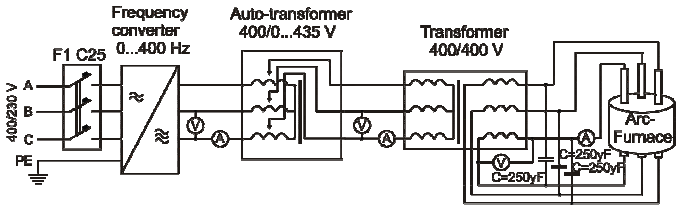

Fig. 20. Scheme of the pioneer experimental set-up, salt solution at AC voltage, frequency 50 Hz.

Fig. 21. Photo of the pioneer experimental set-up.

Fig. 22. Fan, lowered into the salt solution.

However, the salt solution became relatively warm due to currents in it, which means that thermal circulation arose in the furnace. This is why turning of the fan cannot be used as a parameter in the calculations.

Second test was made by hanging the pickup coil between supply electrodes. As the magnetic flux linkage of the imaginary contour in the salt solution is very difficult to measure, some simplifications have to be made. Namely, the imaginary contour in the salt solution has to be replaced by a real contour above the salt solution between the electrodes, as shown in Fig. 23.

From theoretical calculations it can be concluded that induced electromotive force in the contour is very small. To raise the electromotive force to a measurable value, 10 turns of winding was added to the given contour and the dimensions of the contour were chosen so that the induced voltage could be measured with a millivoltmeter. At the parameters of 3.5 A and 50 Hz in the

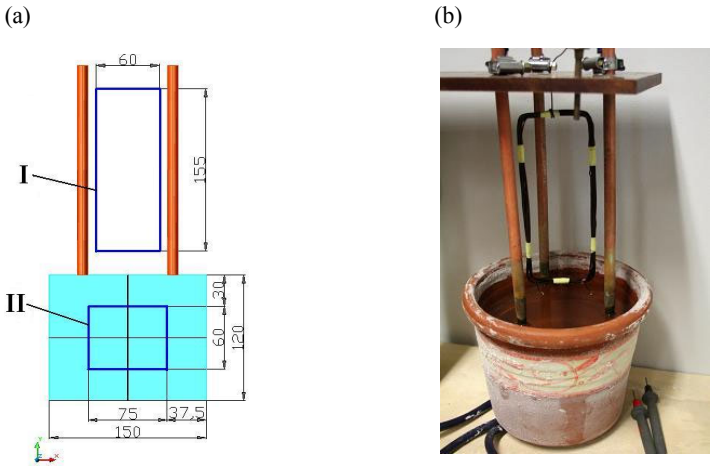

Fig. 23. Placements of the upper contour I and lower contour II (a); photo of the constructed real contour (b).

furnace, the measurements showed 370 mV of induced electromotive force E_1. Calculating the induced voltage in secondary winding of the transformer as

$$E_1 = 4.44 f w_1 \phi_1, \tag{19}$$

the magnetic flux can be obtained as

$$\phi_1 = \frac{E_1}{4.44 f w_1}, \tag{20}$$

where w_1 is the number of turns in the upper contour (in this case 10 turns). Magnetic flux through the contour is

$$\phi_1 = A_1 B_m, \tag{21}$$

where A_1 is the area of the upper contour I. In case of the contour dimensions as shown in Fig. 23, the magnetic flux becomes 1.6×10^{-4} Wb. The average magnetic flux through plane A_1 can be calculated as

$$B_m = \frac{\phi_1}{A_1}. \tag{22}$$

Magnetic flux density is 1.85×10^{-2} T. These calculation results can be transformed to the contour II that is placed in the salt solution. Assumption is made that currents through the salt solution are flowing between upper and lower electrodes. For this the value of the longer side of contour II is multiplied by the value of the shorter side. Resulting area is 4.5×10^{-3} m^2 and denoted as A_{II}. Magnetic flux through the lower contour can be calculated as

$$\phi_{II} = A_{II} B_m, \tag{23}$$

giving as the result 8.33×10^{-5} Wb. Having calculated the magnetic flux through the contour II, induced electromotive force in the same contour can be calculated as well:

$$E_2 = 4.44 f w_2 \phi_{II}, \tag{24}$$

where in that case $w_2 = 1$. Value of the electromotive force is 18.5 mV. When resistivity of the salt ρ is known, then using the length of contour II, resistance of the contour can be calculated as

$$R_2 = \frac{\rho l_{II}}{\sum S}, \tag{25}$$

where $\sum S$ is the area of the cross-section; we get resistance of 6.21 Ω. Now it becomes possible to calculate the current in contour II:

$$I_2 = \frac{E_2}{R_2}. \tag{26}$$

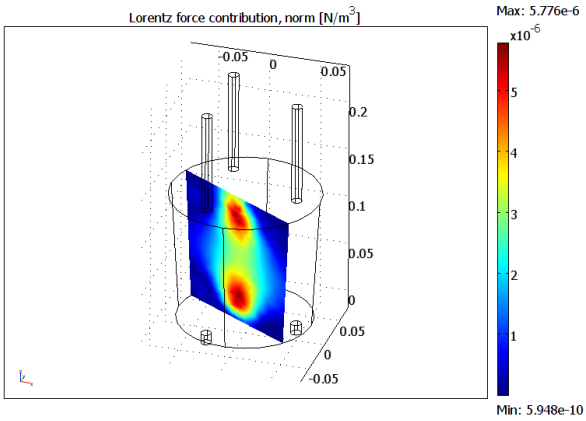

Fig. 24. Three-dimensional force density calculation of the experimental set-up.

Current value of 2.97 mA gives the opportunity to calculate the torque T that is affecting the windings:

$$T = B_m A_{\text{II}} I_2. \tag{27}$$

When the frequency is 50 Hz and current is 3.5 A, resulting torque is 2.48×10^{-7} Nm. Dividing the torque by the arm of the force or the shorter side of the salt solution contour, we obtain $F = 3.62 \times 10^{-6}$ N.

To evaluate the simplified results of the calculations, comparison of modelling results in three-dimensional and two-dimensional calculation are to be made.

Figure 24 shows that calculations of the experimental setup are close to the calculations of the model. Modelling results show that as the height of the salt solution has about a similar value to its width, two maximum points of force density are created in the middle of the salt solution. This can be explained by the fact that the current trajectories of the electrodes float in space, resulting in a higher current density at the upper and lower electrodes.

4. CONCLUSIONS

The preliminary modelling results show that forces, created in the molten metal using this given arc furnace construction, are sufficient to create the mixing process. Force densities become the higher the closer to the electrode the measuring point is, becoming as high as 7467 N/m^3 in case of 40 kA current and 2 Hz frequency. This can be explained by the fact that induced current densities are higher also near the electrodes as shown in Fig. 7.

Optimal mixing frequency requires an in-depth study from the practical point of view, as the slip of the molten metal plays a huge role. Assumptions can be made that the optimal mixing frequency is between 0 and 5 Hz. It is important to

note that in case of higher supply frequency also higher induced currents arise, resulting in higher current densities. As a drawback, slip starts to rise as the frequency is rising.

Arc between the electrode and molten metal plays a huge role as well, because arc pushes molten metal to the bottom of the furnace. Also thermal convections arise in the molten metal, which this paper did not take into account, but which need a further study in the future.

The first constructed pioneer experimental set-up showed that the mixing processes in the salt solutions were created, but whether they arouse because of the thermal convection or Lorentz forces, is hard to say. It is clear that the experimental set-up needs further improvement and modelling has to include additional thermal convections with κ–ε Navier–Stokes [8] liquid viscosity calculations besides the calculations of the Lorentz forces.

REFERENCES

1. Boulet, B., Lalli, G. and Ajersch, M. Modeling and control of an electric arc furnace. In *Proc. American Control Conference*. Denver, Colorado, 2003.
2. Toulouevski, Y. and Zinurov, I. *Innovations in Electric Arc Furnaces*. Springer-Verlag, Berlin, Heidelberg, 2010.
3. Järvik, J., Janson, K. and Mõlder, H. Patent application: Method for stirring molten metal and electric arc furnace. Owner: Tallinn University of Technology. Priority number: P201100014. Priority date: 04.03.2011.
4. Kim, W. and Yoon, J. Numerical prediction of electromagnetically driven flow in ASEA-SKF ladle refining straight induction stirrer. *Ironmaking and Steelmaking*, 1991, **18**, 446–453.
5. Pal, M., Eriksson, R. and Jönsson P. A computational fluid dynamics model of a 20 Kg induction stirred laboratory scaled ladle. In *Proc. COMSOL Multiphysics User's Conference*. Stockholm, KTH, 2005.
6. Larsen, H. Current distribution in the electrodes of industrial three-phase electric smelting furnaces. In *Proc. 2006 Nordic COMSOL Conference*. Copenhagen, 2006. CD-ROM.
7. McDougall, I. Finite element modeling of electric currents in AC submerged arc furnaces. In *Proc. 11th International Congress on Ferroalloys*. The Indian Ferro Alloy Producers' Association, Delhi, India, 2007, vol. 2, 630–637.
8. Foias, C., Rosa, R., Manley, O. and Teman, R. *Navier-Stokes Equations and Turbulence*. Cambridge University Press, Cambridge, 2001.

Vedelmetalli segamise meetod ja vastav kaarleekahi

Heigo Mõlder, Jaan Järvik, Kuno Janson, Rauno Gordon
ja Toomas Vaimann

Vedelmetalli segamise meetod ja sellele vastav kaarleekahi võimaldavad juhtida sulametalli segamist. Segamine toimub vedelmetalli läbivate voolude ja nende põhjustatud magnetväljade koostoimel. Sealjuures tekitatakse elektroodide paigutuse ja nende kaudu sulametalli antavatele vooludele vahelduvkomponentide lisamisega pöörlev magnetväli. Viimane tekitab sulametallis induktsioon-

voolud, mis omakorda kutsuvad sulametallis esile liikumapanevad jõud. Elektroodide toiteallikaid juhitakse juhtsüsteemi abil, mis võimaldab sulatusprotsessi algul kasutada alalisvoolu, ja hiljem, kui metall on juba sulanud, lisada juurde segamisefekti tekitav vahelduvkomponent. Artiklis on esitatud sulametallis tekkivate magnetväljade ja jõutiheduste modelleerimis- ning katsetulemused.